Prepared in cooperation with the National Park Service

Geologic Map of the Valdez D-1 and D-2 Quadrangles (Mount Wrangell Volcano), Alaska

By D.H. Richter, R.G. McGimsey, K.A. Labay, M.A. Lanphere, R.B. Moore, C.J. Nye, D.S. Rosenkrans, and G.R. Winkler

Pamphlet to accompany

Scientific Investigations Map 3351

2016

U.S. Department of the Interior
U.S. Geological Survey

U.S. Department of the Interior
SALLY JEWELL, Secretary

U.S. Geological Survey
Suzette M. Kimball, Director

U.S. Geological Survey, Reston, Virginia: 2016

Suggested citation:
Richter, D.H., McGimsey, R.G., Labay, K.A., Lanphere, M.A., Moore, R.B., Nye, C.J., Rosenkrans, D.S., and Winkler, G.R., 2016, Geologic map of the Valdez D-1 and D-2 quadrangles (Mount Wrangell Volcano), Alaska: U.S. Geological Survey Scientific Investigations Map 3351, 20 p., scale 1:63,360, http://dx.doi.org/10.3133/sim3351.

ISSN 2329-132X (online)

Contents

Figures

Tables

Map Sheet

Geologic Map of the Valdez D-1 and D-2 Quadrangles (Mount Wrangell Volcano), Alaska

By D.H. Richter, R.G. McGimsey, K.A. Labay, M.A. Lanphere, R.B. Moore, C.J. Nye, D.S. Rosenkrans, and G.R. Winkler

Geologic Note

Mount Wrangell (elev. 4,317 m) is the youngest and only active volcano in the Oligocene to Holocene-aged Wrangell volcanic field that extends from beyond the Alaska-Yukon border northwest through the Wrangell Mountains to the Copper River Basin. The volcano is a very large (900 km^3; Nye, 1983) broad shield containing an ice-filled, nonexplosive, collapse caldera measuring 3.2 by 5.6 kilometers. Three known craters, the West, North, and East occur along the north and west margins of the caldera; the caldera is open to the southeast. The volcano is best exposed on its southwest flank (this map area) where a number of deep glaciated canyons cut through hundreds of meters of shield lava flows creating routes for younger, valley-filling lava flows. The shield extends north into the Gulkana A-1 quadrangle (Richter and others, 1994), northeast into the Nabesna A-6 quadrangle (Richter and others, 1997), and east into the McCarthy quadrangle (MacKevett, 1978) where it is almost entirely covered by ice. The present extent of the Mount Wrangell shield showing the entire caldera and locations of the three summit craters is depicted in figure 1.

Mount Wrangell was built rapidly beginning about 650 ka by the outpourings of hundreds of voluminous lava flows from a vent, or vents, apparently in the present summit area. By 200 ka to 300 ka, activity waned and only an occasional lava flow coursed down the glacially carved valleys radiating from the summit or flowed over the upper summit area above the heads of the glacial valleys. The youngest dated valley-fill lava flow is approximately 25,000 years old; one or two undated flows may be younger.

In historical times there have been several reports of lava flows issuing from the summit area. The most reliable and convincing of these were two independent observations (Powell, 1900; Rice, 1900) from Copper Center, Alaska on September 3, 1899 that described great earth movements (the 1899 Yakutat Bay earthquake; Tarr and Martin, 1912) followed by an eruption at Mount Wrangell's summit, consisting of vigorous ash emission and flowing lava on the volcano's northwest flank. This eruptive activity apparently continued for several years after the earthquake, as a photo taken around 1901–02 by Mendenhall and Schrader (1903) shows a large part of Mount Wrangell's summit blanketed by ash. During this study, no evidence of young lava flows in the region were found, although it is very possible that a small-volume flow could be entirely hidden by snow and ice in the 100 years since the event. However, abundant juvenile andesitic pumice (no. 73 on map) was found on the upper Chetaslina Glacier, strongly supporting a very young pyroclastic eruption.

In addition to the 1899–1902 eruptions there have been accounts of strong ash-producing activity on at least four different occasions (Clarke and others, 1989): 1912, July 3, 1921, April 6, 1930, and February 20, 1982. Of these, the 1921 activity was the most spectacular, and possibly erupted from the northeast side of the summit caldera (Clarke and others, 1989).

Present activity is limited to fumaroles in North and West Crater at the summit, at the summit ridge near East Crater, and at two localities at an elevation of 3,657 m on the southwest flank. The summit fumaroles frequently give rise to visible steam plumes (Neal and others, 2014), and occasionally sporadic explosive phreatic activity in North and West Crater will put a thin dusting of ash on the summit ice. The summit area and craters are described by Benson and Motyka (1979) and Benson and Follett (1986).

This study was directed toward Mount Wrangell volcano and the older Wrangell volcanic field rocks that underlie the volcano. These older lavas include the Chetaslina lavas (867 ka–1,650 ka) and a basaltic andesite–dacite center (1,590 ka–1,640 ka) whose source areas are not well defined. Older Paleozoic and Mesozoic sedimentary, igneous, and metamorphic rocks of the Wrangellia terrane underlie the entire Wrangell volcanic field. These old basement rocks, as shown on this map, are taken directly from Winkler and others (1995); further information on these rocks is available from Winkler and others (1981) and Richter and others (2006).

Radiometric ages listed under map letters A, G, H, I, R, X, and Y (table 2) have been previously reported (Nye, 1983); all other ages are new. The sample at map letter *N* (italicized) is from the Long Valley flow in the contiguous Valdez C-1 quadrangle.

Acknowledgments

This is the final geologic publication of Donald H. Richter, who passed away in 2004 while finalizing this map. Don was our close friend and esteemed colleague, and he is sorely missed. The fieldwork on this mapping project was conducted in 1999 and 2000 with much of the background understanding of the Wrangell volcanic field based on Don’s many years working in the area. We are grateful to Christina Neal and Jim Ratté for their technical reviews of the map, and to Scott Starratt for his review of the geologic names. Carolyn Donlin edited the map. Jackie McIntyre contributed to the initial digital cartography. We extend our sincere appreciation to the staff of the Wrangell-Saint Elias National Park and Preserve, as well as to John Staples and Patty Ryan, owners and proprietors of the Golden Spruce Cabins who, in addition to rooms and meals, provided logistical support for the helicopter and fuel staging. Cindi Preller assisted Don during the final weeks of his work on the map and transferred all the materials to the coauthors for completion. Additional colleagues who worked in the area during the project are Chris Waythomas and Kristi Wallace (Chetaslina debris flow), and Jon Hagstrum (paleomagnetic analysis). Andy Calvert provided an $^{40}Ar/^{39}Ar$ age date, and some radiometric ages were determined by D.L. Turner and Nora Shew.

DESCRIPTION OF MAP UNITS

SURFICIAL DEPOSITS

ALLUVIAL DEPOSITS

Qa **Alluvium in streams (Holocene and Pleistocene)—**Includes alluvium in active flood plains and in principal terraces of major, and some minor, streams. Primarily stratified silt, sand, gravel, and boulders

Qaf **Alluvium in fans (Holocene and Pleistocene)—**Mainly large, broad, generally active fans and cones on mountain slopes predominantly along major streams. Primarily sand, gravel, and boulders

Qoa **Older alluvium (Pleistocene)—**Thick inactive fans that have been dissected by modern drainages near the present toes of the Chetaslina Glacier and the East Fork of the Chetaslina Glacier. The deposits are exceptionally well stratified southeast of the toe of the Chetaslina Glacier. Chetaslina lavas (unit Qcl) are exposed in the unit and it is not clear whether the lavas are interbedded in the alluvium or overlain by alluvium. Primarily sand, gravel, and boulders; may include some diamicton. Maximum thickness about 150 m

COLLUVIAL DEPOSITS

Qc **Colluvium, undivided (Holocene and Pleistocene)—**Primarily talus but includes deposits of small landslides, rock glaciers, and other mass-wasting processes. Includes a large proportion of alluvium in small fans and cones and reworked glacial deposits. Shown mainly where deposits cover pre-Cenozoic bedrock and Quaternary volcanic rocks, and locally where deposits mantle steep slopes of older glacial deposits (unit Qog). Not shown, but present, on the steep valley walls of the Chetaslina, East Fork of the Chetaslina, and Cheshnina Rivers where the rivers have incised the glaciolacustrine deposits of the Copper River Basin (unit Qlg). Primarily poorly sorted silt, sand, gravel, and boulders

GLACIAL DEPOSITS

Qr **Rock glacier deposits (Holocene)—**Includes deposits in active rock glaciers that have well-defined lobate and tongue-shaped forms, small coalescing rock glaciers that form linear ridges along bases of steep slopes, and largely inactive rock glaciers with smooth surfaces. Primarily angular blocks and diamicton

Qag **Drift of Alaskan glaciation (Holocene)—**Includes end and lateral moraines of the younger and older phases of Alaskan glaciation, deposited after recession of existing glaciers. Diamicton, local gravel, and sand

Qyg **Drift of younger (Wisconsin) glaciation (Pleistocene)—**Well-defined lateral moraines high on the valley walls of the Dadina, Chetaslina, and East Fork of the Chetaslina Rivers. Diamicton

Qog **Drift of older (Wisconsin and older?) glaciation (Pleistocene)—**Ground moraine extensively modified by alluvial and colluvial processes. Includes at least two interbedded lava flows from Mount Wrangell (unit Qwv). Diamicton; locally alluvial sand, gravel, and boulders

GLACIOLACUSTRINE DEPOSITS

Qlg **Deposits of the Copper River basin, undivided (Pleistocene)—**Primarily diamicton interbedded with stratified lacustrine sediments of glacial Lake Atna (Ferrians, 1989), but unit includes older glacial, lacustrine, and fluvial deposits that underlie the late Pleistocene glacial lake. The diamicton interbedded in the lake sediments ranges from nonsorted till to deposits of poorly sorted material that show graded bedding. The lake sediments, consisting of sand, silt, and clay, locally contain ice-rafted dropstones (Ferrians, 1989). The contact between these mixed glacial and lacustrine deposits and upland drift (unit Qog) and Pleistocene volcanic and older bedrock is arbitrarily shown as a long dashed line at an elevation of about 2,450 ft above sea level, the approximate elevation of the prominent upper strand line of glacial Lake Atna in the eastern part of the Copper River Basin (Ferrians, 1989). Interbedded within the unit in the southwest part of the map area are the Chetaslina debris flow (unit Qcf), a pyroclastic flow (unit Qpf, 342 ka, map letter BB), and at least one lava flow from Mount Wrangell (unit Qwv, 430 ka, map letter H). An overlying subaerial Mount Wrangell lava flow (unit Qwv, 76 ka, map letter L) suggests that glacial Lake Atna had emptied, or was very shallow, by 76 ka. Diamicton, gravel, sand, silt, and clay

QUATERNARY VOLCANIC AND SEDIMENTARY ROCKS

MOUNT WRANGELL VOLCANO

Mount Wrangell volcano (Holocene and Pleistocene, 0.65 Ma and younger)—Mount Wrangell is a large broad shield whose summit area contains a nonexplosive, ice-filled caldera. The lavas of the Mount Wrangell shield show a remarkable relatively uniform major element chemical composition (fig. 2) over a time span of more than 600,000 years. With only minor exceptions, the lavas are highly porphyritic, two-pyroxene, high-silica andesites whose silica content ranges from 60.0 to 63.3 percent. Mount Wrangell shield may be unique having been built by these relatively viscous flows of andesite.

Qwc **Pyroclastic deposits of the Mount Wrangell West Crater (Holocene)—**No attempt was made during this study to examine the fragmental and (or) pyroclastic deposits associated with the West Crater. Samples collected from the summit craters by R.B. Forbes, G.B. Wharton, and C.S. Benson of the University of Alaska, Fairbanks, during 1961–67 are altered andesite flows, breccias, and tuffs. One of these samples from the East Crater (4 km northeast of the map area in the Gulkana A-1 quadrangle, see fig. 1) is described by Furst (1968) as an altered, olivine-bearing, two-pyroxene andesite

Qwv **Mount Wrangell valley-fill and basin lavas (Holocene and Pleistocene)—**Moderately to highly porphyritic, two-pyroxene high-silica andesite flows mineralogically and chemically (60.9–63.6 percent SiO_2, map nos. 29–49 [Note that nos. 31 and 32 are from the contiguous Valdez C-1 quadrangle]) identical to Mount Wrangell shield lavas. Flows traveled down the deeply incised glacial valleys that radiate from the summit ice field on the shield and out into the Copper River Basin where they are interbedded with basin sediments (unit Qlg). Two flows range from about 6 m to more than 100 m thick (116 ka and 378 ka, map letter N and Q) that apparently built up behind ice dams. Well-developed, vertical, and highly contorted columnar joints are common in both; the degree of contortion suggests ice contact conditions. Ice contacts are also indicated by glassy hyaloclastite breccias at the base and margins of some flows. Two of the flows (81 ka and 105 ka, map letters M and K) in the East Fork of the Chetaslina River show inflated pahoehoe surfaces that are mantled by thin scattered glacial deposits.

At least 14 separate flows have been recognized in the East Fork of the Chetaslina River valley and at least four separate flows in the Cheshnina River valley. Where a contact is discernible a long dashed line represents the contact between individual flows. Whole-rock K-Ar ages of the flows (map letters G–Q; except for N, which is on Valdez C-1 quadrangle) range from 25 ka to 430 ka. Age results for these flows are shown as a boxed bold number. Two disparate dates (270 ka and 378 ka, samples 79cnc-1 and 00MC-2) were obtained on what was thought to be a single flow. Either the dates indicate two separate flows or, if a single flow, a measure of the reliability of the K-Ar method for young andesitic lavas. The longest (50 km) and very likely the largest of the late valley flows (116 ka) from Mount Wrangell, which is referred to as the Long Glacier flow, came down the Cheshnina River valley, spread out and thickened to more than 100 m probably behind an ice dam in the Copper River Basin. Most of this flow, including the terminus, is in the adjacent Valdez C-1 and C-2 quadrangles, where the age date (letter N, table 2) and chemistry (nos. 31 and 32, table 1) samples were collected (see fig. 1)

Qwu **Mount Wrangell lavas, undivided (Holocene and Pleistocene)**—Restricted to exposures in unvisited nunataks on the upper slopes of Mount Wrangell above the heads of glacial valleys. Ages possibly as young as a few thousand years

Qw **Lava flows of the Mount Wrangell shield (Pleistocene)**—Medium to dark gray, moderately to highly porphyritic, two-pyroxene, high-silica andesite flows containing phenocrysts of plagioclase (10–50 percent, as much as 6 mm), orthopyroxene (1–6 percent, as much as 4 mm), clinopyroxene (1–7 percent, as much as 3 mm), locally opaque minerals, and an occasional trace of olivine in a glassy, cryptocrystalline, or microcrystalline groundmass. Plagioclase microlites are common in the more crystalline groundmasses. Plagioclase phenocrysts typically occur as single zoned crystals that are euhedral to slightly rounded. Inclusions are common to abundant, especially in interior zones; outermost zones are generally clear. Orthopyroxene tends to be more abundant than clinopyroxene and both, together with plagioclase, are relatively common in crystal clots as much as 6 mm in diameter. SiO_2 content is restricted to a relatively narrow range of 60.0 to 62.5 percent (map nos. 1–23). Whole-rock K-Ar ages range from 90 to 662 ka (map letters A–F, CC). Individual flows range from 3 to more than 20 m thick and generally show fragmented and scoriaceous tops and bottoms. Crudely developed columnar joints are locally common. No volcaniclastic rocks were observed. Maximum total thickness about 750 m.

In the rugged isolated area covered by Mount Wrangell lavas between the East Fork of the Chetaslina and the main Chetaslina Rivers the flows are predominantly porphyritic high-silica andesites typical of other Mount Wrangell lavas. Locally, however, at the base of the unit, but not differentiated on the geologic map, are aphanitic to microporphyritic and slightly porphyritic flows not observed elsewhere on the Mount Wrangell shield. The microporphyritic flows contain 1–5 percent microphenocrysts (<1 mm) of plagioclase, traces of both orthopyroxene and clinopyroxene, and an occasional highly altered crystal of hornblende in a glassy to cryptocrystalline groundmass. SiO_2 content ranges from 62.2 to 63.3 percent (map nos. 24–28), slightly higher than the stratigraphically higher and typical porphyritic flows elsewhere on the shield. The one slightly porphyritic flow observed contains phenocrysts of plagioclase (1–3 percent, as much as 2 mm) and olivine (1–4 percent, as much as 3 mm) in a groundmass of aligned plagioclase microlites. The whole-rock age of this flow is 662 ka (map letter C) suggesting that these aphanitic to microporphyritic and slightly porphyritic flows represent some of the initial lavas of Mount Wrangell. Possibly some of these flows may also be products of a small eruptive center associated with the nearby “Tusk” plug (unit Qwp).

A series of three or four very thick (locally >30 m) flows capping the high plateau between the Cheshnina River and Long Glacier are physically distinct and younger (90 ka, map letter E) than most of the observed Mount Wrangell shield lavas. They are differentiated on the geologic map by a dashed line. The flows contain phenocrysts of plagioclase, orthopyroxene, and clinopyroxene and contain 62.0 percent SiO_2 (map no. 6), all features similar to other shield lavas. However, the flows are much thicker and lighter in color (medium gray) than most shield lavas. Individual flows show well-developed ramp structures and the group unconformably overlies thinner and older Mount Wrangell shield lavas.

As shown, unit Qw may include younger valley-fill lavas (unit Qwv) low in the valley walls of the East Fork of the Chetaslina River from the toe of the East Fork glacier downstream a distance of 5 to 6.5 km. Hyaloclastite deposits are locally exposed in a few side drainages in this area but exposures are poor owing to mantling by colluvium and they are not differentiated on the map

Qwp **Andesite plug of Mount Wrangell (Pleistocene)—**A sharp andesite spire, about 40 meters high, referred to as “Tusk”, intrudes lavas of Mount Wrangell shield (unit Qw) near the terminus of the Chetaslina Glacier. The rock is a medium gray, plagioclase-rich, porphyritic andesite containing phenocrysts of fresh, euhedral plagioclase (60–80 percent, as much as 3 mm), clinopyroxene (4–6 percent, as much as 3 mm), and orthopyroxene (3–5 percent, as much as 2 mm) in a cryptocrystalline groundmass. SiO_2 content is 62.4 percent (map no. 71). The plug may be a source of a few nearby aphanitic to microporphyritic flows (not identified on map) exposed at base of enclosing lavas of Mount Wrangell shield. Whole-rock K-Ar age is 529 ka (map letter S)

Qwe **Early lava flows of Mount Wrangell (Pleistocene)—**Exposed at the base of a 750-m section of lava flows of Mount Wrangell shield, north of the Chetaslina Glacier, and in three isolated localities as single flows within Pleistocene glacial deposits (unit Qog). The flows north of the Chetaslina Glacier, which form a distinct unit as much as 150 m thick, are porphyritic, olivine-bearing, two-pyroxene andesites that show magma mixing features and contain 54.3 to 58.5 percent SiO_2 (Nye, 1983). The isolated flows are also olivine-bearing two-pyroxene porphyritic to seriate andesites; one flow contains 57.4 percent SiO_2 (map no. 50). A flow low in the section north of the Chetaslina Glacier yielded a K-Ar age of 690 ka (map letter R)

MOUNT DRUM VOLCANO

Qda **Nadina volcanic avalanche, landslide, and glacial deposits, undivided (Pleistocene)—**Variegated, crudely stratified and poorly sorted juvenile bombs, pumice, ash and blocks of andesite and dacite that resulted from paroxysmal explosive activity within the central vent area of Mount Drum (Richter and others, 1979). Deposits are locally covered by, and mixed with, glacial drift

Qdl **Andesite flows (Pleistocene)—**Medium to dark gray, porphyritic, olivine-bearing andesite lava flows containing phenocrysts of plagioclase (10–15 percent, as much as 3 mm), fresh olivine (4–6 percent, as much as 3 mm), and orthopyroxene (2–3 percent, as much as 1 mm) in a cryptocrystalline groundmass. SiO_2 content is 60.8 percent (map no. 72). In adjacent northern quadrangle (Gulkana A-2), some flows also contain clinopyroxene and hornblende (Richter and others, 1979). Flows are thick (>10 m) and may have a source in the vicinity of the Snider Peak dome on Mount Drum, 8 km to the north

VOLCANICLASTIC DEPOSITS

Qcf **Chetaslina volcanic debris flow (Pleistocene)—**Multi-colored, voluminous (7–12 km^3) debris avalanche deposit containing megablocks, as much as 90 m in maximum dimension, of both porphyritic and aphanitic andesite lava, hydrothermally altered lava, volcanic breccia, pyroclastic flow deposits, lacustrine sediments, and glacial deposits. Unit underlies a 270-ka Wrangell lava flow (map letter G, unit Qwv) and probably is younger than a 342-ka pyroclastic flow (map letter BB, unit Qpf) in the valley of the East Fork of the Chetaslina River. Although the debris flow is not in contact with the pyroclastic flow, bombs apparently from the pyroclastic flow occur in the debris flow. The maximum thickness is about 100 m. The deposit’s source is equivocal: originally thought to be related to a summit collapse of Mount Wrangell (Yehle and Nichols, 1980), later Richter and others (1995) suggested that the deposit was a result of the cataclysmic eruption that destroyed the top of Mount Drum. More recently, Waythomas and Wallace (2002) concluded that the deposit is associated with a sector collapse of Mount Wrangell’s flank in the area of the Chetaslina lavas (unit Qcl). However, the age of lava flows that once covered this potential source area (map letter C) casts doubt on that interpretation

Qpf **Pyroclastic flow (Pleistocene)**—Pale to medium yellowish brown pyroclastic flow deposit containing abundant bombs, scoria, and pumice as much as 15 cm in diameter. Analyses of five scoria and pumice clasts suggest a bimodal andesite-dacite distribution (60.0–61.4 percent SiO_2 and 65.8–66.9 percent SiO_2; C. Waythomas, unpub. data, 2001). A whole-rock K-Ar age of 342 ka was obtained on a scoria bomb (map letter BB). Unit forms spires and hoodoos; maximum thickness is about 20 m. Exposed only near the confluence of the Chetaslina and East Fork of the Chetaslina Rivers, it is interbedded with glaciolacustrine and glacial deposits (unit Qlg) of the Copper River Basin. Chemical composition suggests that Mount Drum, 37 km to north, is a more likely source than Mount Wrangell

BASALTIC ANDESITE–DACITE CENTER

Located between the Dadina and Chichokna Rivers, small eruptive center(s) unconformably overlies both, the Jurassic granodiorite of the Chitina batholith (unit Jc) and lava flows possibly from the roughly contemporaneous Chetaslina center (unit Qcl). Rocks consist of a series of dacite domes, plugs, block and ash deposits, andesite and basaltic andesite flows. Source of the flows is unknown, however, whole-rock K-Ar ages suggest that these flows and domes are related in time to the Chetaslina lavas, representing pre-modern Wrangell volcanism.

Qah **Andesite flows (Pleistocene)**—Medium gray, slightly to moderately porphyritic andesite flows containing phenocrysts of plagioclase (1–20 percent, as much as 3 mm), orthopyroxene (trace–5 percent, as much as 3 mm), hornblende (trace–5 percent, as much as 3 mm), and traces of clinopyroxene and olivine in a cryptocrystalline to plagioclase (< 0.5 mm) rich groundmass. The plagioclase is generally clean and euhedral. Orthopyroxene grows in clots with the plagioclase and as single crystals. The hornblende is generally altered to black oxide minerals. SiO_2 content for two flows (map nos. 51 and 55) ranges from 59.2–62.5 percent. Whole-rock K-Ar age is 1,590 ka (map letter U). Flows as much as 30 m thick; maximum thickness of unit is probably less than 300 m

Qdc **Dacite debris apron (Pleistocene)**—Blocks and smaller fragments of hornblende dacite in crudely layered deposits that dip away from the associated plug spire

Qdi **Dacite plugs (Pleistocene)**—Light gray, moderately porphyritic hornblende dacite plugs containing phenocrysts of plagioclase (5–20 percent; as much as 3 mm), hornblende (4–8 percent; as much as 2 mm), and traces of orthopyroxene in a cryptocrystalline to microcrystalline groundmass. Plagioclase is generally euhedral with inclusion-rich centers and clear rims; hornblende has pronounced black oxide rims. The larger of the two plugs forms a prominent inaccessible spire near north edge of map area. This plug's sample was obtained from talus (unit Qdc). Both plugs contain 65.1 percent SiO_2 (map nos. 52, 53); the smaller plug yielded a K-Ar age of 1,640 ka (map letter T)

Qd **Dacite flow dome (Pleistocene)**—A light gray porphyritic hornblende dacite dome containing phenocrysts of plagioclase (10–15 percent, as much as 3 mm) and hornblende (3–5 percent, as much as 2 mm) that is locally rimmed with black oxides, in a cryptocrystalline groundmass. SiO_2 content is 64.6 percent (map no. 54). The dome, which appears to be one massive flow, is more than 200 m thick

Qba **Basaltic andesite flows (Pleistocene)—**Dark gray, slightly porphyritic basaltic andesite flows containing phenocrysts of olivine (3–5 percent, as much as 4 mm), in clots and as individual rounded crystals, a trace of clinopyroxene in a cryptocrystalline groundmass consisting of 70–80 percent plagioclase laths, as much as 1 mm long. SiO_2 content is 53.7 percent (map no. 56). Unit consists of only 2 to 4 thin (5–8 m) flows; maximum thickness is probably less than 30 m

Qdb **Dacite block and ash deposit (Pleistocene)—**Contains primarily light gray, porphyritic dacite blocks as much as 2 m in diameter in a matrix of light gray to very light gray ash. The blocks contain phenocrysts of fresh and euhedral plagioclase (15–20 percent, as much as 4 mm), hornblende (1–3 percent, as much as 1 mm), orthopyroxene (2–4 percent, as much as 2 mm) and rounded clinopyroxene (1–2 percent, as much as 2 mm) in a cryptocrystalline groundmass. SiO_2 content of dacite block is 65.0 percent (map no. 57)

SHALLOW INTRUSIVE ROCKS

Qod **Dacite intrusion (Pleistocene)—**Light olive-gray to greenish-gray, porphyritic dacite intrusion, containing phenocrysts of plagioclase, hornblende (mostly altered), and biotite in a cryptocrystalline groundmass locally flooded by calcite. Exposed in two small areas along northern margin of quadrangle west of Chichokna River. Description from principal exposure to the north in the Gulkana A-1 quadrangle where unit intrudes older andesite flows of the Chetaslina lavas and where biotite yielded K-Ar age of 1,350 ka (Richter and others, 1994)

CHETASLINA LAVAS

Originally named the “Chetaslina vent” lavas by Nye (1983) for a sequence of andesite flows that underlie, and are chemically and mineralogically distinct from, the Mount Wrangell shield lavas. Unit consists primarily of andesite lava flows and breccias, dacite-andesite domes, and pyroclastic deposits that locally show the effects of very strong hydrothermal alteration. However, existence of a major central vent system was not confirmed. Whole-rock K-Ar ages indicate that the lavas were erupted between 1,650 and 874 ka.

Qci **Andesite dikes (Pleistocene)—**Two dikes, of the five observed, were accessible and sampled. Both are dark-gray, slightly porphyritic andesite. The freshest appearing dike contains phenocrysts of plagioclase, orthopyroxene, and clinopyroxene in a microcrystalline groundmass of plagioclase laths. The mineralogy and chemistry (61.3 percent SiO_2, map no. 59) of this dike and its age (545 ka, map letter V) suggests an affinity with Mount Wrangell rather than the Chetaslina lavas. The other dike (55.9 percent SiO_2, map no. 60) contains phenocrysts of plagioclase (5 percent, as much as 3 mm) and clinopyroxene (2 percent, as much as 1 mm) in a microcrystalline groundmass of plagioclase laths, opaque minerals, and green clay minerals

Qcd **Andesite-dacite lava domes(?) and breccias (Pleistocene)—**Light gray coalescing domes(?) ranging from holocrystalline-seriate (crystal mush) andesite to porphyritic dacite. The crystal mush (62.0 percent SiO_2, map no. 67) contains plagioclase (75–90 percent, from <1 mm to as much as 5 mm), orthopyroxene (3–8 percent, as much as 2 mm), clinopyroxene (1–2 percent, as much as 2 mm), and olivine (trace amounts to 1 percent, <1 mm as small rounded prisms). The porphyritic dacite (64.8 percent SiO_2, map no. 62) contains phenocrysts of plagioclase (6–20 percent, as much as 4 mm), clinopyroxene (trace amounts to 4 percent, as much as 2 mm), orthopyroxene (1–3 percent, as much as 3 mm), and hornblende (trace amounts to 1 percent, as much as 3 mm) in a cryptocrystalline groundmass. Exposed rocks range from massive, dome-like units, as much as 40 m thick, to extremely fragmental units, interpreted as carapace breccias, containing blocks as much as a few meters in diameter. The unit is largely covered by talus. Whole-rock K-Ar age is 874 ka (map letter W)

Qcl **Lava flows, pyroclastic deposits, and breccias, undifferentiated (Pleistocene)—**Primarily a variety of dark brownish-gray andesite lava flows ranging from holocrystalline-seriate flows to porphyritic flows, pyroclastic fall deposits, and breccias. A holocrystalline-seriate flow (55.7 percent SiO_2, map no. 64) contains plagioclase (70–80 percent, as much as 4 mm), orthopyroxene (1–3 percent, as much as 3 mm) both as single crystals and in clots, olivine (1–3 percent, as much as 3 mm) altered to a brownish clay(?) mineral and minor interstitial material. The porphyritic flows (55.3–62.9 percent SiO_2, map nos. 61, 63, 68–70) contain phenocrysts of plagioclase (5–40 percent, as much as 6 mm), orthopyroxene (3–10 percent, as much as 3 mm), clinopyroxene (1–4 percent, as much as 3 mm), and occasional olivine (0–3 percent) in an altered cryptocrystalline groundmass. One highly porphyritic flow (60.8 percent SiO_2, map no. 65) also contains as much as 1 percent fresh biotite in clusters as much as 2 mm in diameter and 1 percent black oxide ghosts of hornblende crystals. Weakly indurated, light green, mauve, and cream colored pyroclastic fall(?) deposits locally form a landscape of spires and hoodoos that easily break down into a mud-rich slurry. A few laharic(?) breccias were noted during aerial observation of the more rugged area of the Chetaslina terrain. One possible vent breccia (64.3 percent SiO_2, map no. 66) contains abundant clasts of plagioclase porphyry and small (<5 mm) clasts of fine-grained siltstone or chert in a matrix of broken plagioclase crystals, altered hornblende laths, clinopyroxene, and altered cryptocrystalline material. Nye (1983) reported whole-rock K-Ar ages of 1,580 ka and 980 ka for andesitic lava flows in this unit (map letters X and Y); two additional whole-rock K-Ar ages of 1,650 ka (map letter Z) and 867 ka (map letter AA) were obtained during this study

SEDIMENTARY ROCKS

Qcg **Conglomerate (Pleistocene)—**Slightly indurated pebble to boulder fluvial conglomerate with interbedded lenses of sandstone. Appears to fill a paleo-valley on Chetaslina lavas (unit Qcl). This conglomerate is a continuation of a more extensive sedimentary rock unit mapped in the contiguous Gulkana A-1 quadrangle (Richter and others, 1994)

MESOZOIC AND PALEOZOIC ROCKS

The distribution of these basement rocks, as shown on the geologic map, is taken with minor modification from Winkler and others (1981, 1995); the descriptions, with minor additions, are taken from Winkler and others (1995).

Ks **Marine sedimentary rocks (Early Cretaceous)—**Consists of the Berg Creek Formation and unnamed marine sedimentary rocks. Primarily glauconitic and fossiliferous siltstone, sandstone, and conglomerate

Jc **Chitina Valley batholith (Late Jurassic)—**Weakly to strongly foliated quartz monzodiorite, quartz diorite, tonalite, and granodiorite

JTRc **Marine clastic and carbonate rocks, undivided (Late or Middle Jurassic to Late Triassic)—**Consists of the Kotsina Conglomerate (Late or Middle Jurassic), the lower member of the McCarthy Formation (Late Triassic), and the Chitistone and Nizina Limestones (Late Triassic). The Kotsina Conglomerate is a thick-bedded cobble to pebble conglomerate containing lenses of sandstone, siltstone, and carbonaceous shale. The lower member of the McCarthy Formation consists of impure limestone, shale, and chert that gradationally overlies thin- and thick-bedded limestones of the Chitistone and Nizina Limestones

JIPm **Haley Creek metamorphic assemblage (Late Jurassic and Pennsylvanian or older?)—**Consists of the Uranatina River metaplutonic unit (Jurassic and Pennsylvanian) and the Strelna Metamorphics of Plafker and others (1989) (Early Pennsylvanian and older?). Low- to medium-grade (greenschist to amphibolite facies) metamorphic rocks tentatively considered to represent roots of Skolai magmatic arc

TRn **Nikolai Greenstone (Late and (or) Middle Triassic)—**Chiefly subaerial tholeiitic flood basalts

PIPs **Skolai Group (Early Permian and Pennsylvanian)—**Volcanic, volcaniclastic, and sedimentary rocks of a late Paleozoic magmatic arc

References Cited

Benson, C.S., and Follett, A.B., 1986, Application of photogrammetry to the study of volcano-glacier interactions on Mount Wrangell, Alaska: Photogrammetric Engineering and Remote Sensing, v. 52, no. 6, p. 813–827.

Benson, C.S., and Motyka, R.J., 1979, Glacier-volcano interactions on Mt. Wrangell, Alaska: Fairbanks, University of Alaska, Annual Report, Geophysical Institute p. 1–25.

Clarke, G.K.C., Cross, G.M., and Benson, C.S., 1989, Radar imaging of glaciovolcanic stratigraphy, Mount Wrangell caldera, Alaska—Interpretation model and results: Journal of Geophysical Research, v. 94, p. 7,237–7,249.

Ferrians, O.J., Jr., 1989, Glacial Lake Atna, Copper River Basin, Alaska, *in* Carter, L.D., Hamilton, T.D., and Galloway, J.P., eds., Late Cenozoic history of the interior basins of Alaska and the Yukon: U.S. Geological Survey Circular 1026, p. 85–88.

Furst, M.J., 1968, The reconnaissance petrology of andesites from the Mt. Wrangell caldera, Alaska: Fairbanks, University of Alaska, M.S. thesis, 83 p.

MacKevett, E.M., Jr., 1978, Geologic map of the McCarthy quadrangle, Alaska: U.S. Geological Survey Miscellaneous Investigations Series Map I–1032, scale 1:250,000.

Mendenhall, W.C., and Schrader, F.C., 1903, The mineral resources of the Mount Wrangell district, Alaska: U.S. Geological Survey Professional Paper 15, 71 p.

Neal, C.A., Herrick, J., Girina, O.A., Chibisova, M., Rybin, A., McGimsey, R.G., and Dixon, J., 2014, 2010 volcanic activity in Alaska and Kamchatka—Summary of events and response of the Alaska Volcano Observatory: U.S. Geological Scientific Investigations Report 2014–5034, 76 p.

Nye, C.J., 1983, Petrology and geochemistry of Okmok and Wrangell volcanoes, Alaska: Santa Cruz, University of California, Ph.D. dissertation, 208 p.

Plafker, G., Nokleberg, W.J., and Lull, J.S., 1989, Bedrock geology and tectonic evolution of the Wrangellia, Peninsular, and Chugach terranes along the Trans-Alaska Crustal Transect in the Chugach Mountains and southern Copper River basin, Alaska: Journal of Geophysical Research, v. 94 p. 4,255–4,295.

Powell, A.M., 1900, The Gakona and Chistochina Rivers, *in* United States Congress, Senate Committee on Military Affairs, Compilation of narratives of explorations in Alaska: Washington, D.C., Government Printing Office, p. 783.

Rice, J.F., 1900, From Valdez to Eagle City, *in* United States Congress, Senate Committee on Military Affairs, Compilation of narratives of explorations in Alaska: Washington, D.C., Government Printing Office, p. 788.

Richter, D.H., Duffield, W.A., Sawyer, D.A., Ratté, J.C., and Schmoll, H.R., 1994, Geologic map of the Gulkana A-1 quadrangle, south-central Alaska: U.S. Geological Survey Geologic Quadrangle Map GQ–1728, scale 1:63,360.

Richter, D.H., Moll-Stalcup, E., Duffield, W.A., and Shew, Nora, 1997, Geologic map of the Nabesna A–6 quadrangle, Alaska: U.S. Geological Survey Open File Report 97–475, scale 1:63,360.

Richter, D.H., Preller, C.C., Labay, K.A., and Shew, N.B., compilers, 2006, Geologic map of the Wrangell-Saint Elias National Park and Preserve, Alaska: U.S. Geological Survey Scientific Investigations Map 2877, scale 1:350,000.

Richter, D.H., Rosenkrans, D.S., and Steigerwald, M.J., 1995, Guide to the volcanoes of the western Wrangell Mountains, Alaska—Wrangell-St. Elias National Park and Preserve: U.S. Geological Survey Bulletin 2072, 31 p.

Richter, D.H., Smith, R.L., Yehle, L.A., and Miller, T.P., 1979, Geologic map of the Gulkana A-2 quadrangle, Alaska: U.S. Geological Survey Geologic Quadrangle Map GQ–1520, scale 1:63,360.

Tarr, R.S., and Martin, Lawrence, 1912, The earthquakes at Yakutat Bay, Alaska in September, 1899: U.S. Geological Survey Professional Paper 69, 135 p.

Waythomas, C.F., and Wallace, K.L., 2002, Flank collapse at Mount Wrangell, Alaska, recorded by volcanic mass-flow deposits in the Copper River lowland: Canadian Journal of Earth Sciences, v. 39, p. 1257–1279.

Winkler, G.R., Goldfarb, R.J., and Borden, J.C., 1995, Map showing geology and geochemically anomalous areas, Valdez 1° × 3° quadrangle, south-central Alaska, *in* Goldfarb, R.J., Borden, J.C., and Winkler, G.R., Geochemical survey of the Valdez 1° × 3° quadrangle, south-central Alaska: U.S. Geological Survey Bulletin 2084, scale 1:250,000.

Winkler, G.R., Silberman, M.L., Grantz, Arthur, Miller, R.J., and MacKevett, E.M., Jr., 1981, Geologic map and summary geochronology of the Valdez quadrangle, southern Alaska: U.S. Geological Survey Open-File Report 80–892–A, 2 sheets, scale 1:250,000.

Yehle, L.A., and Nichols, D.R., 1980, Reconnaissance map and distribution of the Chetaslina volcanic debris flow (new name), southeastern Copper River Basin and adjacent areas, south-central Alaska: U.S. Geological Survey Miscellaneous Field Studies Map MF–1209, scale 1:250,000.

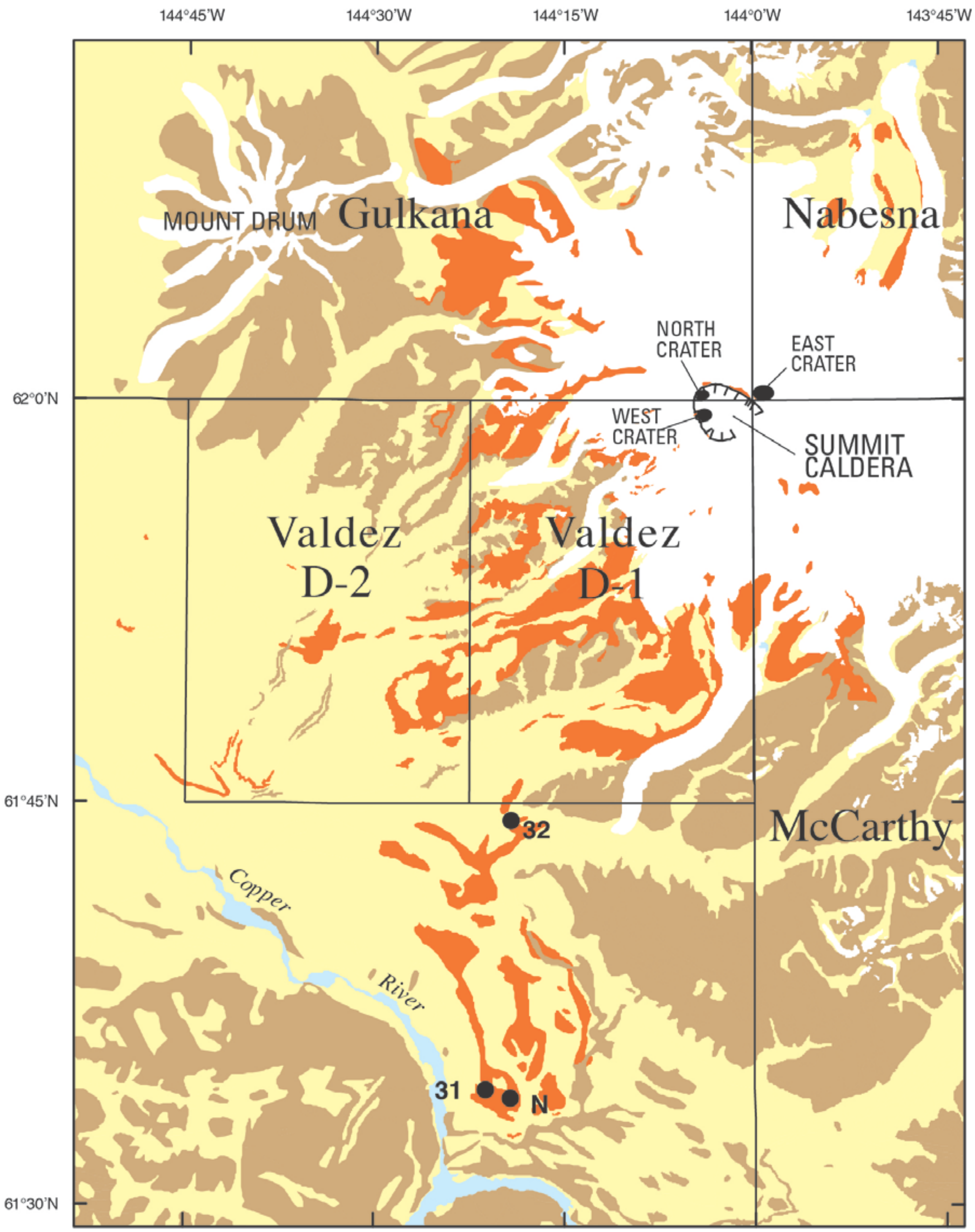

Figure 1. Generalized map showing present extent of Mount Wrangell lavas (red), Valdez D-1 and D-2 quadrangles, and sample locations (dots) outside Valdez D-1 and D-2 map area. All other rocks are tan, surficial deposits are yellow, ice is white, and rivers are blue.

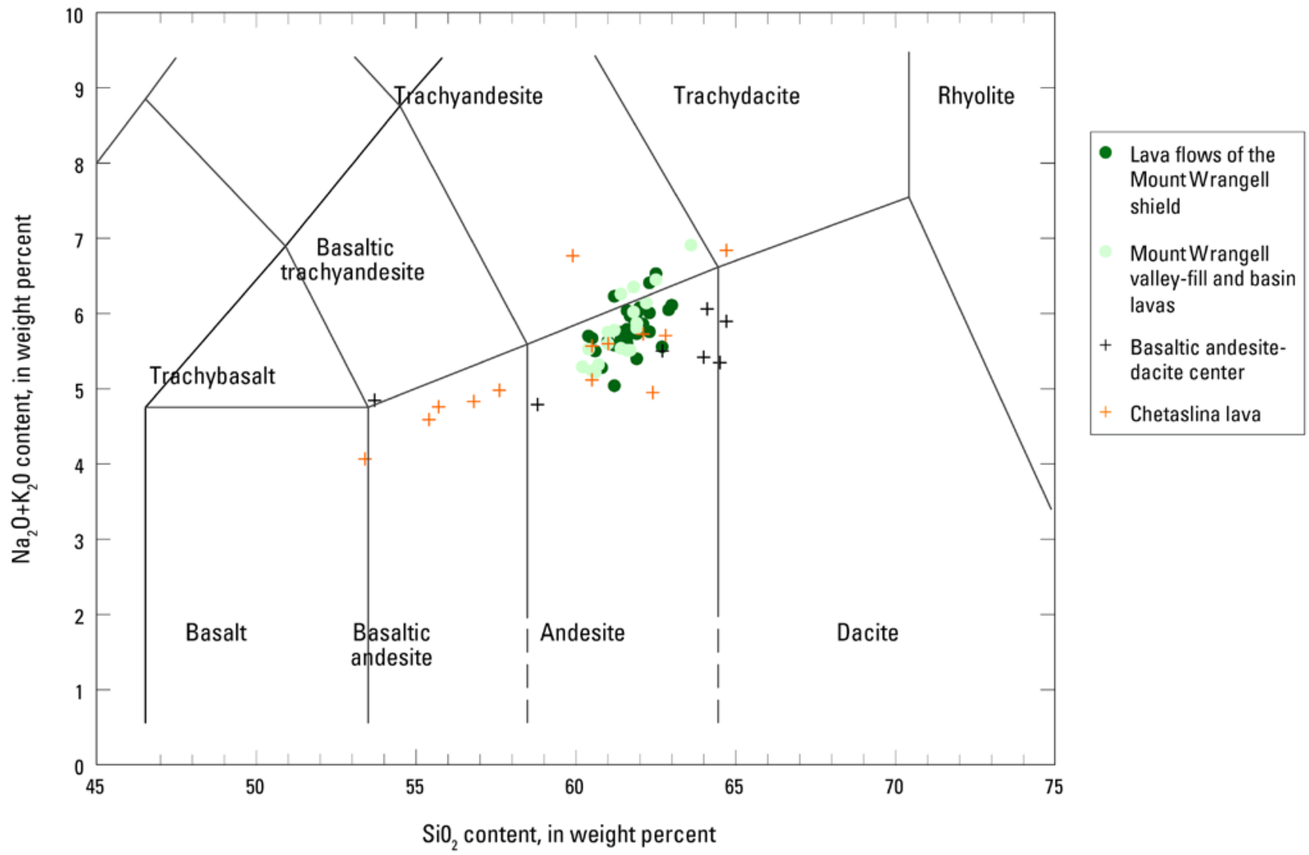

Figure 2. Total alkalis (Na_2O+K_2O) versus silica content for volcanic rocks from the Valdez D-1 and D-2 quadrangles, Alaska.

Table 1. Chemical analyses of volcanic rocks from the Valdez D-1 and D-2 quadrangles, Alaska.

[Analyses by U.S. Geological Survey x-ray fluorescence methods, D. Siems, analyst. Data are normalized volatile-free; %, percent, LOI, lost on ignition. Samples of map numbers *31* and *32* are from the contiguous Valdez C-1 quadrangle; see fig. 1]

Map no.	Field no.	$\%SiO_2$	$\%Al_2O_3$	$\%FeTO_3$	%MgO	%CaO	$\%Na_2O$	$\%K_2O$	$\%TiO_2$	$\%P_2O_5$	%MnO	LOI	Original total	Latitude_NAD27	Longitude_NAD27
							Lava flows of the Mount Wrangell shield (unit Qw)								
1	99ARh-1	62.2	16.3	5.59	3.24	5.38	3.76	2.34	0.88	0.24	0.09	0.85	99.65	61.836775	-144.430902
2	99ARh-3	62.0	16.2	5.70	3.37	5.41	3.77	2.31	0.89	0.25	0.09	0.88	99.34	61.849147	-144.346688
3	99ARh-4	61.9	16.7	5.61	3.03	5.54	3.95	2.05	0.89	0.26	0.09	0.03	100.02	61.858423	-144.249289
4	99ARh-21	62.2	15.9	5.77	3.42	5.35	3.72	2.35	0.90	0.24	0.09	0.85	99.28	61.814307	-144.362716
5	99ARh-34	61.6	16.7	5.76	3.16	5.67	3.99	1.97	0.90	0.26	0.09	0.12	100.24	61.846570	-144.130270
6	99ARh-35	62.0	16.8	5.84	2.19	5.37	4.27	2.11	1.02	0.28	0.08	<0.01	100.45	61.851872	-144.100505
7	99ARh-36A	60.0	16.3	6.37	4.24	6.01	3.72	1.95	0.98	0.27	0.10	<0.01	100.59	61.885998	-144.058912
8	99ARh-36B	60.5	16.4	5.77	4.35	6.10	3.75	1.92	0.82	0.27	0.09	0.45	99.97	61.888485	-144.055729
9	99ARh-38	61.7	16.3	5.84	3.50	5.59	3.77	2.06	0.88	0.25	0.10	<0.01	100.62	61.859030	-144.015503
10	99ARh-39	62.4	16.6	5.80	2.15	5.10	4.35	2.17	1.04	0.30	0.08	0.26	100.12	61.868942	-144.089600
11	99ARh-50	60.6	17.1	5.93	3.59	6.11	3.74	1.76	0.80	0.23	0.09	0.20	99.95	61.908267	-144.188244
12	99ARh-51	61.5	16.3	5.99	3.37	5.64	3.93	1.97	0.89	0.26	0.10	<0.01	100.46	61.880195	-144.162325
13	00ARh-1	62.2	16.5	5.65	3.13	5.49	3.64	2.10	0.87	0.27	0.09	0.83	98.66	61.974834	-144.347116
14	00ARh-3	62.3	16.2	5.69	3.38	5.34	3.50	2.36	0.88	0.25	0.09	0.79	98.84	61.799234	-144.416363
15	00ARh-6B	62.2	17.1	5.73	2.26	5.40	3.94	2.06	1.00	0.29	0.08	0.16	100.19	61.843060	-144.102813
16	00ARh-9	60.9	17.4	5.79	3.55	6.28	3.59	1.42	0.72	0.27	0.10	0.03	100.53	61.829225	-144.117022
17	00ARh-10	61.7	16.9	5.60	3.04	5.69	3.78	2.00	0.90	0.29	0.09	0.12	99.48	61.817767	-144.164045
18	00ARh-13	61.8	17.1	5.37	3.18	5.85	3.67	1.96	0.81	0.25	0.08	0.39	99.08	61.793159	-144.113714
19	00ARh-14	62.3	16.9	5.23	2.95	5.64	3.66	2.10	0.83	0.27	0.08	0.30	99.32	61.783035	-144.155463
20	00ARh-15D	61.0	17.0	5.88	3.61	6.05	3.51	1.78	0.81	0.25	0.09	0.12	99.72	61.928401	-144.169873
21	00ARh-21	62.5	16.7	5.42	3.15	5.60	3.67	1.88	0.73	0.27	0.09	-0.04	100.25	61.979877	-144.234252
22	00ARh-36	62.1	16.6	5.59	3.32	5.45	3.53	2.21	0.87	0.26	0.09	0.02	100.29	61.812396	-144.410406
23	00ARh-37	61.9	16.9	5.43	3.21	5.77	3.64	2.00	0.83	0.26	0.09	0.73	99.52	61.798683	-144.236696
24	99ARh-46	63.3	17.2	4.79	2.47	5.24	3.95	2.19	0.62	0.19	0.08	0.84	99.55	61.918012	-144.290253
25	99ARh-46A	62.9	16.6	5.23	2.78	5.30	4.02	2.03	0.80	0.24	0.08	0.06	99.98	61.921715	-144.290973
26	00ARh-17	62.3	16.9	5.11	3.65	5.75	3.81	1.62	0.61	0.21	0.08	0.49	99.43	61.933666	-144.263651
27	00ARh-17A	62.2	16.4	5.78	3.09	5.45	3.77	2.03	0.92	0.28	0.09	0.62	99.38	61.932315	-144.254155
28	00ARh-29	62.5	16.6	5.47	2.96	5.48	3.71	2.06	0.85	0.26	0.09	0.89	98.59	61.932315	-144.254155

Map no.	Field no.	%SiO_2	%Al_2O_3	%$FeTO_3$	%MgO	%CaO	%Na_2O	%K_2O	%TiO_2	%P_2O_5	%MnO	LOI	Original total	Latitude_NAD27	Longitude_NAD27
45	00ARh-32	62.0	16.4	5.79	3.46	5.56	3.55	2.05	0.84	0.27	0.09	1.20	98.98	61.867509	-144.307267
Mount Wrangell valley-fill and basin lava (unit Qwv)															
29	99ARh-5	60.9	17.0	5.89	3.54	6.01	3.80	1.82	0.82	0.23	0.09	0.06	100.24	61.871938	-144.239077
30	99ARh-22	61.4	17.1	5.82	2.34	5.72	4.18	2.07	1.01	0.28	0.08	0.62	99.74	61.764326	-144.678139
31	*99ARh-24*	61.6	16.5	5.68	3.42	5.74	3.87	1.97	0.84	0.23	0.09	0.01	100.44	61.572031	-144.344307
32	*99ARh-25*	61.7	16.7	5.61	3.35	5.72	3.82	1.97	0.83	0.24	0.09	0.11	100.30	61.724658	-144.312002
33	99ARh-29	61.4	17.0	5.96	2.28	5.70	4.23	2.03	1.04	0.29	0.09	<0.01	100.02	61.853464	-144.409143
34	99ARh-49	63.6	16.0	5.78	1.78	4.43	4.41	2.50	1.12	0.34	0.08	0.13	100.04	61.893844	-144.276322
35	99ARh-49B	62.4	16.6	5.63	2.32	5.30	4.13	2.30	1.02	0.29	0.08	<0.01	100.22	61.892714	-144.275007
36	99CW-16-1	61.6	16.9	5.93	2.24	5.55	4.24	2.09	1.05	0.30	0.08	0.09	100.35	61.847668	-144.616789
37	00ARh-7	61.6	16.6	5.74	3.56	5.78	3.58	1.93	0.82	0.25	0.09	-0.01	99.95	61.854315	-144.115832
38	00ARh-11	62.4	16.8	5.78	2.21	5.24	4.02	2.14	1.02	0.31	0.08	-0.06	99.63	61.811127	-144.199913
39	00ARh-12	61.6	16.7	5.79	3.55	5.78	3.57	1.93	0.83	0.25	0.09	0.18	100.23	61.789347	-144.341701
40	00ARh-15	61.0	17.0	5.88	3.56	6.05	3.55	1.80	0.80	0.24	0.09	-0.15	99.46	61.909922	-144.173307
41	00ARh-16	60.7	17.1	5.92	3.67	6.18	3.52	1.71	0.80	0.24	0.09	-0.19	99.79	61.940724	-144.188589
42	00ARh-19A	60.9	16.7	5.66	4.15	6.24	3.40	1.87	0.73	0.26	0.09	0.94	99.36	61.899632	-144.278147
43	00ARh-26	60.5	18.0	5.54	2.76	6.42	3.78	1.78	0.89	0.28	0.08	-0.06	100.79	61.864780	-144.344218
44	00ARh-27	61.0	17.1	5.82	3.51	6.06	3.55	1.81	0.81	0.25	0.09	0.89	98.73	61.861634	-144.329258
46	00Mc-1	61.1	16.4	6.14	3.80	5.75	3.46	2.13	0.90	0.26	0.10	0.84	98.90	61.787685	-144.687394
47	00Mc-2	61.1	17.5	5.72	2.60	6.06	3.83	1.94	0.96	0.29	0.09	0.49	100.23	61.845670	-144.575096
48	00Mc-6	61.7	17.0	5.91	2.34	5.64	3.96	2.05	1.03	0.31	0.09	-0.12	100.16	61.857053	-144.476964
49	00Mc-8	61.8	16.4	5.77	3.37	5.55	3.57	2.26	0.91	0.25	0.09	1.03	98.69	61.790347	-144.388087
Early Wrangell lava (unit Qwe)															
50	99ARh-30	57.4	16.3	6.93	5.58	6.93	3.33	2.08	0.99	0.33	0.11	0.04	99.98	61.894815	-144.455661
Basaltic andesite–dacite center (units Qdi, Qd, Qah, Qba, Qdb, Qdc)															
51	00ARh-35	59.2	17.7	6.54	3.90	6.60	3.75	1.07	0.80	0.32	0.11	0.95	99.34	61.993355	-144.469528
52	00ARh-5	65.1	17.2	4.12	2.21	5.02	3.91	1.61	0.50	0.21	0.07	1.74	98.24	61.985265	-144.420422
53	00ARh-38	65.1	17.0	4.13	2.56	5.09	4.10	1.30	0.45	0.21	0.07	0.51	99.05	61.997437	-144.469470
54	99ARh-16	64.6	17.2	4.26	2.32	5.00	4.15	1.74	0.50	0.19	0.08	0.21	100.17	61.957773	-144.478846
55	00ARh-4A	62.5	17.0	5.42	2.95	5.49	3.84	1.64	0.78	0.29	0.09	-0.08	100.37	61.972338	-144.489955
56	99ARh-17A	53.7	16.1	8.39	6.79	8.31	3.35	1.50	1.32	0.40	0.13	0.23	99.99	61.989096	-144.486966
57	99ARh-17	65.0	17.2	4.15	1.90	4.85	4.37	1.77	0.50	0.20	0.07	1.41	98.68	61.991325	-144.477399
Chetaslina lava (units Qci, Qcd, Qcl)															
58	00ARh-39	57.7	17.7	6.68	4.66	7.07	3.49	1.50	0.78	0.26	0.11	0.51	99.81	61.942863	-144.310637

Map no.	Field no.	%SiO_2	%Al_2O_3	%$FeTO_3$	%MgO	%CaO	%Na_2O	%K_2O	%TiO_2	%P_2O_5	%MnO	LOI	Original total	Latitude_NAD27	Longitude_NAD27
59	00ARh-33A	61.3	16.8	5.64	3.91	6.12	3.42	1.76	0.75	0.25	0.09	1.17	98.77	61.937059	-144.229123
60	00ARh-23A	55.9	18.7	8.14	3.80	7.33	3.83	0.43	1.39	0.38	0.07	4.05	95.54	61.997131	-144.420959
61	99ARh-48B	62.9	17.3	4.95	2.70	5.53	4.17	1.54	0.65	0.20	0.08	0.15	99.92	61.910364	-144.326228
62	99ARh-8	64.8	16.0	5.16	1.64	4.12	4.48	2.38	0.90	0.35	0.09	0.34	99.78	61.895112	-144.364564
63	99ARh-10	55.3	18.2	7.64	4.93	7.80	3.78	0.95	1.00	0.27	0.12	<0.01	100.66	61.890393	-144.379562
64	99ARh-15	55.7	18.1	7.48	4.80	7.87	3.68	0.94	1.00	0.29	0.12	0.94	99.43	61.914477	-144.356427
65	00ARh-18A	60.8	15.8	5.36	4.05	5.72	3.94	2.93	0.89	0.37	0.08	1.95	98.49	61.911093	-144.277549
66	00ARh-23B	64.3	16.8	4.77	2.52	5.51	3.41	1.69	0.66	0.24	0.06	2.46	96.99	61.996851	-144.425325
67	99ARh-9	62.0	17.2	5.52	2.98	5.52	4.03	1.69	0.76	0.24	0.09	0.06	100.17	61.892638	-144.373396
68	00ARh-23D	57.8	16.6	6.53	5.46	7.14	3.37	1.55	1.03	0.39	0.11	1.19	98.21	61.993140	-144.434742
69	00ARh-31	61.7	16.8	5.79	3.07	5.61	3.73	1.95	0.97	0.33	0.08	1.45	98.11	61.953372	-144.206241
70	00ARh-33	62.4	16.7	5.47	3.15	5.44	3.66	2.06	0.87	0.27	0.07	1.38	97.83	61.939285	-144.232037
Andesite plug of Mount Wrangell (unit Qwp)															
71	99ARh-44	62.4	16.7	5.36	2.89	5.42	3.99	2.04	0.85	0.25	0.09	0.16	99.99	61.939110	-144.315647
Andesite lava flows of Mount Drum (unit Qdl)															
72	99ARh-19	60.8	17.0	5.49	4.58	5.97	3.68	1.58	0.55	0.19	0.09	1.00	99.28	61.979812	-144.671920
Young Wrangell pumice															
73	00ARh-40	60.6	17.1	5.90	3.80	6.23	3.62	1.61	0.79	0.25	0.09	-0.06	99.99	61.981695	-144.242873

Table 2. Radiometric ages from map units in the Valdez D-I and D-2 quadrangles, Alaska.

[Ages listed for map letters A, G, H, I, R, X, and Y have been reported previously (Nye, 1983). All other ages are new. Sample at map letter *N* is from the Long Valley flow in the contiguous Valdez C-1 quadrangle; see fig. 1]

Map letter	Sample no.	K_2O%	$^{40}Ar_{rad}$/gm	$^{40}Ar_{rad}$%	Calc. age (ka)	Analyst	Latitude_NAD27	Longitude_NAD27
			Lava flows of the Mount Wrangell shield (unit Qw)					
A	79cne-29	2.158±0.005	13.00 x 10^{-13}	5.40	420±30	D.L. Turner	61.979949	-144.301892
B	80cnh-16	2.115±0.010	8.45 x 10^{-13}	10.15	280±13	D.L. Turner	61.927152	-144.172793
			8.58 x 10^{-13}	10.27				
C	99ARh-43	0.890±0.006	8.475 x 10^{-13}	5.70	662±45	M.A. Lanphere	61.933666	-144.263651
D	99ARh-51	2.164±0.011	16.08 x 10^{-13}	42.10	516±8	M.A. Lanphere	61.880195	-144.162325
E	00ARh-8	2.422±0.250	3.153 x 10^{-13}	3.50	90±15	M.A. Lanphere	61.832683	-144.110183
F	00ARh-14	2.188±0.013	4.449 x 10^{-13}	1.00	141±59	M.A. Lanphere	61.783035	-144.155463
O	99ARh-36B	2.088±0.004	1.506 x 10^{-13}	1.60	50±13	M.A. Lanphere	61.888485	-144.055729
CC	99ARh-41	2.2975±0.005	4.05 x 10^{-13}	10.92	124.8±5.2	A.T. Calvert	61.860979	-144.092201
			4.19 x 10^{-13}	11.91				
			Mount Wrangell valley-fill and basin lavas (unit Qwv)					
G	79cnc-1	2.043±0.015	7.900 x 10^{-13}	1.80	270±40	D.L. Turner	61.847668	-144.616789
H	79cnd-2	2.014±0.012	12.50 x 10^{-13}	1.80	430±80	D.L. Turner	61.787685	-144.687394
I	79cnf-1	1.943±0.022	2.100 x 10^{-13}	1.30	80±20	D.L. Turner	61.974947	-144.209392
J	80cnh-18	1.820±0.000	0.680 x 10^{-13}	2.98	25±8	D.L. Turner	61.857053	-144.476964
			0.610 x 10^{-13}	2.66				
K	80cnh-19	1.792±0.002	2.790 x 10^{-13}	4.93	105±10	D.L. Turner	61.866162	-144.403092
			2.650 x 10^{-13}	4.68				
L	90ARh-7	1.656±0.005	1.635 x 10^{-13}	2.20	76±15	Nora Shew	61.758436	-144.654839
			2.020 x 10^{-13}	2.30				
M	99ARh-5	1.970±0.003	2.298 x 10^{-13}	4.80	81±9	M.A. Lanphere	61.871938	-144.239077
N	*99ARh-23*	*2.158±0.004*	*3.600 x* 10^{-13}	*6.60*	*116±9*	*M.A. Lanphere*	61.570117	-144.315607
P	00ARh-26	1.891±0.007	3.320 x 10^{-13}	7.30	122±9	M.A. Lanphere	61.864780	-144.344218
Q	00Mc-2	2.014±0.001	11.00 x 10^{-13}	3.80	378±39	M.A. Lanphere	61.845670	-144.575096
			Early lava flows of Mount Wrangell (unit Qwe)					
R	79cne-3	2.233±0.013	22.10 x 10^{-13}	9.60	690±30	D.L. Turner	61.967410	-144.295892
			Andesite plug of Mount Wrangell (unit Qwp)					
S	99ARh-44	2.088±0.007	15.91 x 10^{-13}	57.70	529±7	M.A. Lanphere	61.939110	-144.315647
			Basaltic andesite-dacite center, dacite plugs (unit Qdi)					
T	00ARh-38	1.359±0.004	32.07 x 10^{-13}	48.40	1,640±20	M.A. Lanphere	61.997437	-144.469470

Map letter	Sample no.	K_2O%	$^{40}Ar_{rad}$/gm	$^{40}Ar_{rad}$%	Calc. age (ka)	Analyst	Latitude_NAD27	Longitude_NAD27
Basaltic andesite-dacite center, andesite flow (unit Qah)								
U	00ARh-4A	1.742±0.008	40.00 x 10^{-13}	53.20	1,590±16	M.A. Lanphere	61.972338	-144.489955
Andesite dikes (Chetaslina or Mount Wrangell, unit Qci)								
V	00ARh-33	2.181±0.002	17.10 x 10^{-13}	43.60	545±8	M.A. Lanphere	61.939285	-144.232037
Dacite dome (Chetaslina lavas, unit Qcd)								
W	99ARh-9	1.726±0.003	21.72 x 10^{-13}	66.20	874±10	M.A. Lanphere	61.892638	-144.373396
Lava flows (Chetaslina lavas, unit Qcl)								
X	79cne-1	0.962±0.006	21.80 x 10^{-13}	6.70	1,580±30	D.L. Turner	61.964350	-144.300292
Y	79cnf-2	2.125±0.017	30.10 x 10^{-13}	10.10	980±30	D.L. Turner	61.957716	-144.198970
Z	00ARh-23D	1.514±0.014	37.40 x 10^{-13}	55.00	1,650±17	M.A. Lanphere	61.993140	-144.434742
AA	00ARh-39	1.511±0.010	18.90 x 10^{-13}	8.90	867±38	M.A. Lanphere	61.942863	-144.310637
Pyroclastic flow (unit Qpf)								
BB	90ARh-7A	0.393±0.003	1.885 x 10^{-13}	2.80	342±16	Nora Shew	61.757048	-144.655190
			1.981 x 10^{-13}	3.40				